Intestinal alkaline phosphatase is a gut mucosal defense factor maintained by enteral nutrition

Ross F. Goldberg*, William G. Austen, Jr.*, Xiaobo Zhang*, Gitonga Munene*, Golam Mostafa*, Shaluk Biswas*, Michael McCormack*, Kyle R. Eberlin*, John T. Nguyen*, Hamit S. Tatlidede*, H. Shaw Warren†, Sonoko Narisawa‡, Jose L. Millán‡, and Richard A. Hodin*§

*Department of Surgery, Massachusetts General Hospital, Harvard Medical School, Boston, MA 02114; †Department of Pediatrics, Massachusetts General Hospital, Harvard Medical School, Boston, MA 02114; and ‡Burnham Institute for Medical Research, La Jolla, CA 92037

Communicated by Patricia K. Donahoe, Massachusetts General Hospital, Boston, MA, December 27, 2007 (received for review September 27, 2007)

Under conditions of starvation and disease, the gut barrier becomes impaired, and trophic feeding to prevent gut mucosal atrophy has become a standard treatment of critically ill patients. However, the mechanisms responsible for the beneficial effects of enteral nutrition have remained a mystery. Using *in vitro* and *in vivo* models, we demonstrate that the brush–border enzyme, intestinal alkaline phosphatase (IAP), has the ability to detoxify lipopolysaccharide and prevent bacterial invasion across the gut mucosal barrier. IAP expression and function are lost with starvation and maintained by enteral feeding. It is likely that the IAP silencing that occurs during starvation is a key component of the gut mucosal barrier dysfunction seen in critically ill patients.

gut barrier | lipopolysaccharide | trophic feeding | bacterial translocation | NF-κB

Among the most critical functions of the mammalian gut mucosa is to provide a barrier to luminal microbes and toxins while simultaneously allowing for the necessary digestion and absorption of dietary nutrients. The molecular mechanisms that govern barrier function are incompletely understood, but it is clear that under conditions of starvation and disease, the gut barrier becomes impaired, leading to significant morbidity and mortality (1–8). Trophic enteral feeding to prevent gut mucosal atrophy and resultant barrier dysfunction has become part of the standard treatment of intensive care unit patients (9–14). The mechanism(s) responsible for the beneficial effects of trophic feeding are not understood.

Intestinal alkaline phosphatase (IAP), a brush–border protein that hydrolyzes monophosphate esters, is expressed exclusively in villus-associated enterocytes and is considered an excellent marker for crypt–villus differentiation (15–18). Narisawa *et al.* (19) reported that compared with their wild-type (WT) littermates, mice lacking IAP gained more weight under conditions of a high-fat diet. In addition, several studies have shown that the IAP enzyme is capable of detoxifying LPS, likely through dephosphorylation of the lipid A moiety, the primary source of its endotoxic effects (20). Despite these few reports, the physiological role of IAP within the gut has not been elucidated.

Results and Discussion

To examine the functional role of IAP, we developed *in vitro* model systems using intestinal cell lines (T84, HT-29, and IEC-6) that express little or no IAP under basal conditions. Stable cell lines were created that overexpress IAP (Fig. 1*A*), and enzyme assays were used to determine the cellular localization of the ectopically expressed IAP protein. The results in Fig. 1*B* show that parent cells make little, if any, endogenous IAP. In contrast, large amounts of IAP enzyme are seen in the stably transfected cells. Importantly, the vast majority of the IAP activity is in the membrane fraction as opposed to the cytosol. Fig. 1*C* shows the results of the control experiment used to validate our separation of membranous and cytosolic fractions, confirming that the majority of the MAPK enzyme activity exists within the cytosol rather than the membrane. This membrane localization of IAP is similar to that described *in vivo*, where after fat feeding IAP was detected transferring from the Golgi apparatus to the microvillus membrane (18) and surrounding fat droplets in the villi of the intestinal mucosa (21).

In addition to its membrane localization, it has also been reported that in response to fat feeding *in vivo*, the IAP protein is secreted outside of the cell and into the intestinal lumen (21, 22). We therefore assayed both the cellular extract (cell lysate) and the surrounding media for IAP activity. The results are shown in Fig. 2*A* and reveal again that parent HT-29 cells produce little IAP enzyme, whereas the transfected cells express a large amount of IAP. This IAP activity is present in the cell lysate as expected, but it is also present at high levels in the media, indicating that some of the protein is secreted outside of the cell. The secreted IAP protein (predicted 60 kDa in size) was mostly retained by a 50-kDa cutoff filter but was able to pass through the 100-kDa cutoff filter.

We next determined whether the ectopic IAP expressed in the stable cell lines functions in the same manner as the IAP produced endogenously by intestinal epithelial cells. To address this issue, we examined IAP expression and function in HT-29 cells treated with sodium butyrate, a known inducer of endogenous IAP expression via a mechanism of histone hyperacetylation (23). Fig. 2*C* shows the data on IAP enzyme activity, revealing that endogenous IAP is secreted into the media after 24 h of butyrate treatment, and this activity is similar to that seen in the case of the IAP-expressing stable cell lines. To ensure that the activity being observed was indeed IAP and not another alkaline phosphatase (AP), these same samples were also exposed to phenylalanine, a specific inhibitor of IAP activity. The majority of the observed activity was inhibited in the presence of phenylalanine but not affected by homoarginine (data not shown). All of the data in Figs. 1 and 2 are shown for the HT-29 cells, but the same results were obtained in the two other cell lines, T84 and IEC-6.

To examine the effects of IAP on the LPS pathway, we used immunofluorescence studies to assay NF-κB activation (Fig. 3*A*), staining the RelA/p65 component of the NF-κB protein complex that becomes translocated into the nucleus in response to LPS [4′,6-diamidino-2-phenylindole (DAPI) was used for nuclear staining]. When WT HT-29 and HT-29/vector cells were exposed to LPS, there was a clearly visualized nuclear translocation of the RelA/p65 protein. In contrast, in the case of the HT-29/IAP cells, RelA/p65 nuclear translocation was completely blocked.

LPS sensitivity was further examined by using a well characterized luciferase (Luc) reporter gene regulated by a consensus NF-κB

Author contributions: R.F.G. and W.G.A. contributed equally to this work; R.F.G., W.G.A., H.S.W., and R.A.H. designed research; R.F.G., W.G.A., X.Z., G. Munene, G. Mostafa, S.B., M.M., K.R.E., J.T.N., and H.S.T. performed research; S.N. and J.L.M. contributed new reagents/analytic tools; R.F.G., W.G.A., X.Z., H.S.W., and R.A.H. analyzed data; and R.F.G. and R.A.H. wrote the paper.

The authors declare no conflict of interest.

§To whom correspondence should be addressed. E-mail: rhodin@partners.org.

This article contains supporting information online at www.pnas.org/cgi/content/full/0712140105/DC1.

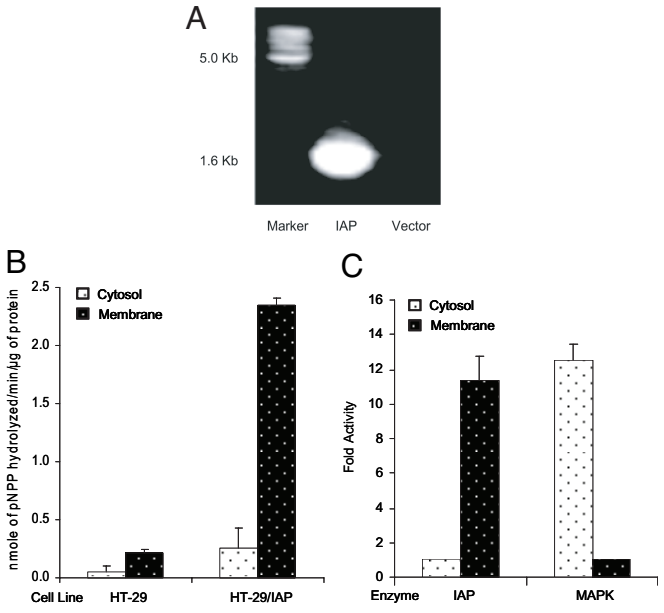

Fig. 1. Localization of the IAP enzyme. (*A*) Gel image of RT-PCR showing IAP mRNA only expressed in the IAP stable transfectant cell line compared with empty vector as a control. (*B*) Cellular fractions were purified to separate the cytosolic and membranous components. IAP activity was determined in the fraction from parent HT-29 and HT-29/IAP stable cell lines. (*C*) IAP and MAPK activity in membranous and cytosolic fractions of HT-29/IAP stable cells. Data are presented as mean ± SD.

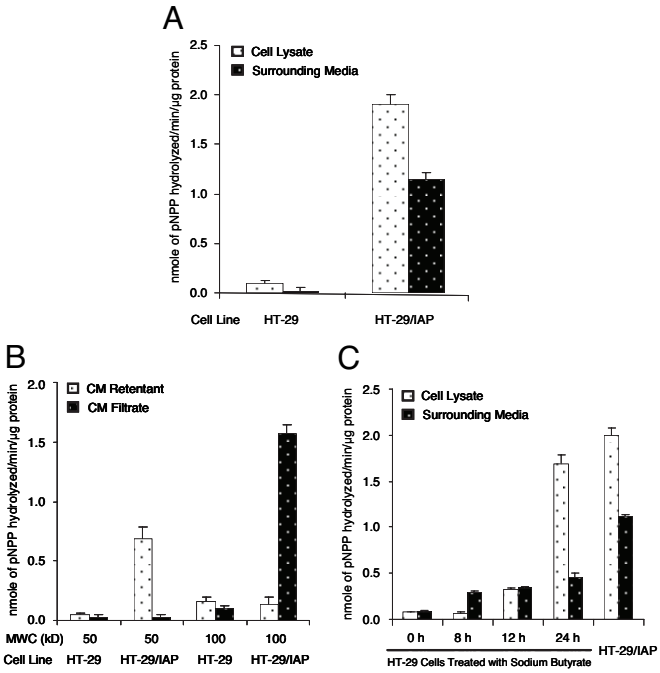

Fig. 2. The IAP enzyme is secreted by the cell. (*A*) IAP enzyme activities are depicted in cell lysate and surrounding medium, comparing the parent and transfected HT-29 cells overexpressing IAP. (*B*) The conditioned medium was filtered through different pore sizes, the results showing that the IAP enzyme is between 50 and 100 kDa (the enzyme is known to be ≈60 kDa in size). (*C*) Endogenous vs. ectopically produced IAP. Cell lysates and conditioned medium were assayed for IAP enzyme activity. Upon treatment with butyrate, endogenous IAP enzyme activity increases in the lysates and the surrounding medium. The activities are similar to that seen in the case of the ectopic IAP produced in the stable cell line (HT29/IAP). Data are presented as mean ± SD.

response element. WT and IAP-expressing IEC-6 cells were transiently transfected with the NF-κB-Luc plasmid and incubated with varying concentrations of LPS and luciferase activity determined after 48 h. Results are shown for the nontransformed cell line, IEC-6, because we have found these cells to be extremely reliable for transient transfections, but similar results were obtained in the other two cell lines. As seen in Fig. 3*B*, NF-κB-Luc was markedly activated in the parent cells, whereas the effects of LPS were almost completely blocked in the IAP-expressing cells. We next interrogated components of the LPS signaling pathway in the nontransformed IEC-6 cells and in the transformed T84 cells to identify the specific site(s) at which IAP works to cause LPS resistance. Western blotting was used to assess the levels of phosphorylated IκBα and RelA/p65, key steps in the NF-κB pathway. It is clear that IAP was able to inhibit the phosphorylation of these two proteins involved in LPS signaling and the NF-κB pathway (Fig. 3 *C* and *D*). In the control cells, both of these proteins become phosphorylated in response to LPS. In contrast, the basal levels of these phosphoproteins are reduced in the IAP cells, and furthermore, their phosphorylation in response to LPS is inhibited.

It is clear from our studies that IAP is able to mediate cellular resistance to LPS. To assess directly the ability of IAP to dephosphorylate LPS, we compared parent and IAP-transfected HT-29 cells. For these experiments, we again used HT-29 cells because of their ability to be induced to make large amounts of endogenous IAP. Under basal conditions, HT-29 cells do not produce much, if any, IAP, so it was not surprising that we saw a minimal amount of LPS-dephosphorylating activity in the parent cells (Fig. 4*A*). Remarkably, high levels of LPS-dephosphorylating activity were seen in the IAP transfectants (HT-29/IAP). The amount of this biological activity differed in the various compartments, the highest levels seen in the whole-cell lysates, followed by the membrane fraction and the conditioned media. The lowest levels were seen in the cytosolic compartment (there was no difference between the parent and IAP-expressing cells). These results indicate that the ectopic IAP protein made in the transfected cells has the ability to dephosphorylate LPS. In addition, we compared the LPS-dephosphorylating activity in the transfected (ectopically produced IAP) and butyrate-treated cells (endogenous IAP) (Fig. 4*B*) and found similar results with regard to the amount and distribution of LPS-dephosphorylating activity. This LPS-dephosphorylating activity was also secreted outside of the cell, a finding that was also seen in the case of endogenous IAP produced in response to butyrate exposure. Based on these data, it appears that LPS detoxification likely occurs in the physiological context of IAP made within an intestinal epithelial cell. Taken together, these *in vitro* studies have shown that an AP enzyme made within a eukaryotic cell is able to detoxify LPS and confer resistance to this bacterial toxin, blocking its signaling and downstream effects.

Based on these *in vitro* data, we sought to examine the physiological role of the IAP protein *in vivo*. We first confirmed the presence of IAP activity and LPS-dephosphorylating activity in the intact gut. It has been shown (18) and confirmed by our laboratory that the majority of IAP enzyme activity *in vivo* is localized to the proximal small intestine (data not shown). WT and IAP knockout (KO) mice were killed, and duodenal mucosal scrapings from each group of animals were studied for IAP activity and LPS-dephosphorylating activity using the *p*-nitrophenyl phosphate (*p*NPP) and the malachite–molybdate substrates, respectively. The WT mice had significantly higher IAP enzyme and LPS-dephosphorylating activities compared with their KO littermates (Fig. 5 *A* and *B*). Other segments of bowel from each animal were also studied, and it was found that the majority of both the IAP and LPS-dephosphorylating activities were located in the duodenum (data not shown). These observations in the intact gut indicate that an endogenous AP enzyme actually functions to detoxify LPS.

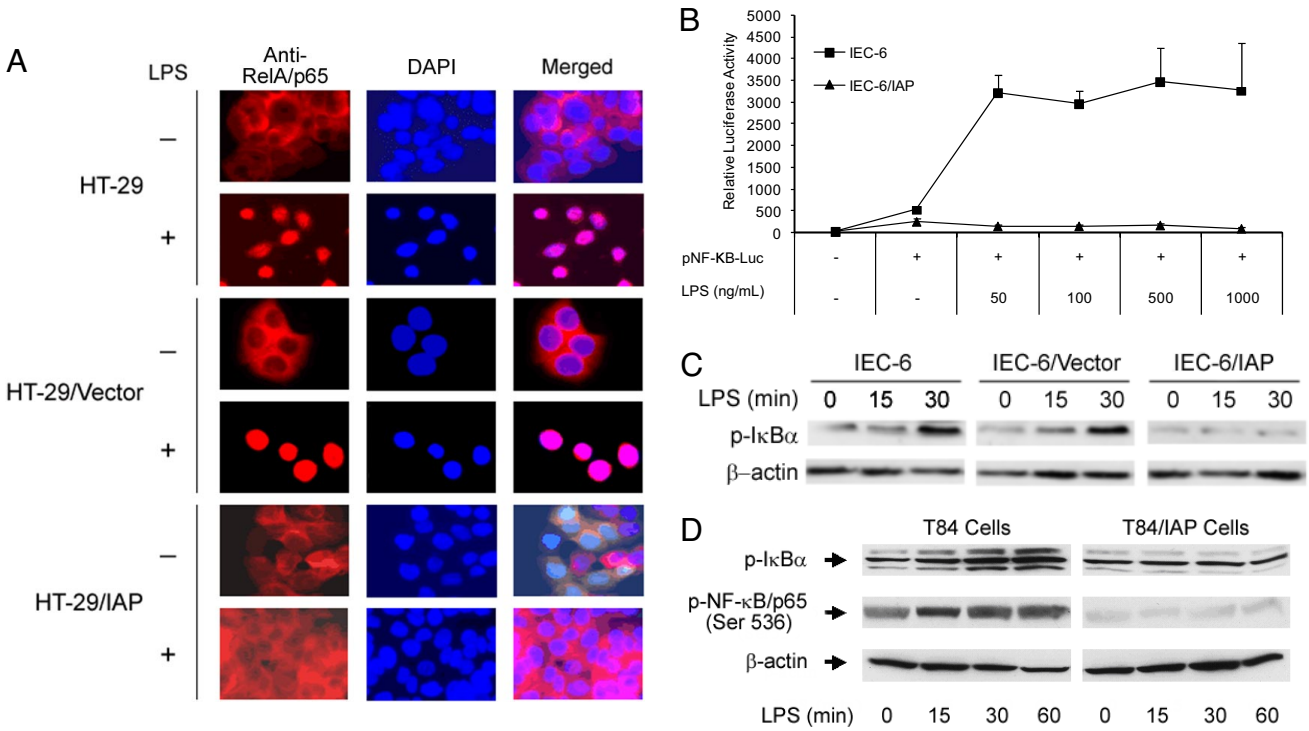

Fig. 3. IAP inhibits the NF-κB pathway. (*A*) IAP blocks LPS-activated NF-κB nuclear translocation. HT-29 WT, vector, and IAP-overexpressing cells were exposed ±LPS, then fixed and stained for immunofluorescence studies. Staining with antibodies for RelA/p65 (part of the NF-κB complex translocated into the nucleus) and DAPI (cell nucleus) is shown. Only the IAP-overexpressing cells were able to block the effects of LPS, preventing NF-κB nuclear translocation. (*B*) IAP protects the cell from LPS exposure. WT and IAP-expressing IEC-6 cells were exposed to LPS at varying concentrations. NF-κB-Luc activity was determined as the readout for the cellular effects of LPS. Data refer to mean ± SD. (*C*) IAP specifically blocks LPS activation of the NF-κB pathway in IEC-6 cells. Western blotting was performed with a specific antibody to IκBα phosphorylation, a critical step in the NF-κB pathway. IkBα did not become phosphorylated in the case of the IAP-overexpressing cells exposed to LPS. The β-actin staining was used to confirm the relative amounts of protein in each sample. (*D*) IAP blocks phosphorylation of components of the NF-κB pathway in LPS-treated T84 cells. Western blotting was performed with specific antibodies to the phosphorylated forms of the IκBα and RelA/p65 proteins. The β-actin staining was used to confirm the relative amounts of protein in each sample.

We and others have reported that IAP expression is lost with starvation (23–25). We therefore placed WT and KO animals on a water-only diet for 2 days and in some cases refed normal chow for another 2 days. Fig. 5 *A* and *B* shows that with starvation, both IAP and LPS-dephosphorylating activities decrease to low levels (similar to those in the KO animals). Starvation had little impact on the LPS-dephosphorylating activity in the KO animals. Interestingly, upon refeeding there was an increase in both IAP and LPS-dephosphorylating activities in the WT animals, indicating that the changes with starvation are reversible. These observations suggest that IAP silencing could result in impairment in the ability of the host to protect itself from luminal LPS exposure.

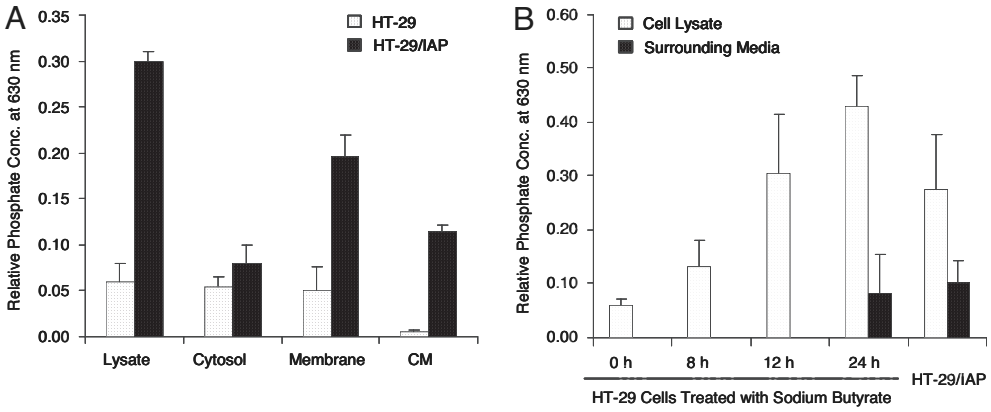

Fig. 4. LPS-dephosphorylating activity. (*A*) Biological activity is present in the transfected but not parent HT-29 cells, the magnitude greatest in the cell lysate > membrane > medium (all significant, $P < 0.01$). There was no statistically significant difference in LPS-dephosphorylating activity in the cytosol between the transfected and parent cells. (*B*) The LPS-dephosphorylating activity is compared in the endogenous (butyrate-treated) and ectopically produced (transfected cells) conditions. The increases in the lysates became significant ($P < 0.01$) at 12 and 24 h of butyrate exposure and in the medium at 24 h. Data are presented as mean ± SD.

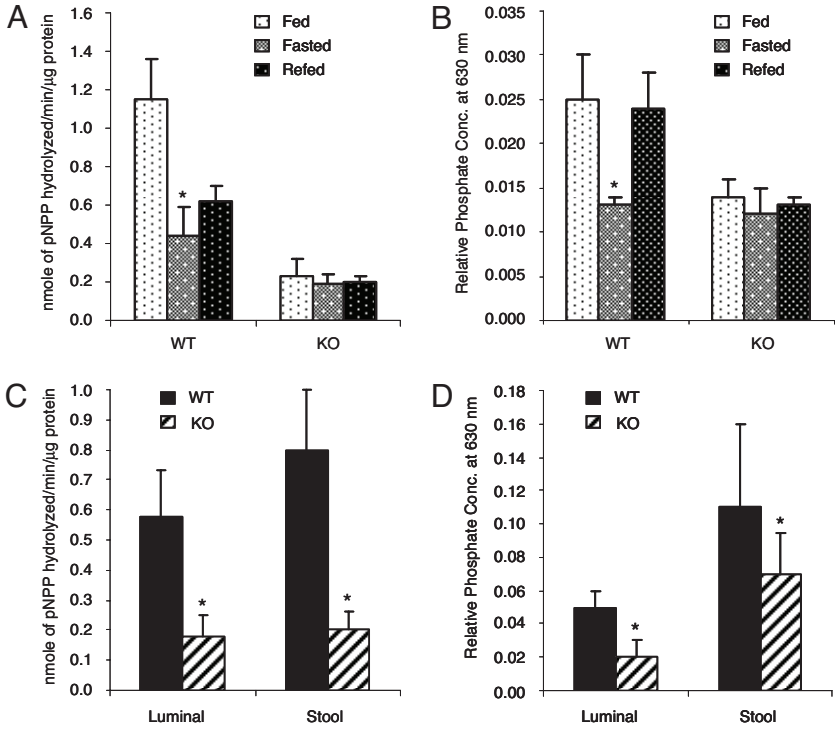

Fig. 5. IAP enzyme dephosphorylates LPS *in vivo*. (*A*) AP assay for WT and IAP KO mice groups that were fed ($n = 5$), fasted (starved for 2 days, $n = 5$), and refed (starved for 2 days, refed for 2 days, $n = 4$). Starvation causes a significant decrease in IAP activity in the WT animals, down to levels similar to those in the KO mice. Refeeding stimulates IAP expression in the WT animals. Starvation and refeeding appear to have minimal effect on IAP expression in the IAP KO mice. *, $P < 0.05$, comparing fasted with the fed and refed WT animals. As expected, KO AP levels are significantly lower than those in the WT animals. (*B*) A similar pattern was seen in the LPS-dephosphorylating activity of the fed, fasted, and refed WT and KO groups. Starvation dramatically reduced the LPS-dephosphorylating ability of the WT animal, whereas refeeding returned it to normal levels. *, $P < 0.05$, comparing fasted with the fed and refed WT animals. KO levels are significantly lower than those in the WT animals. (*C*) A comparison of luminal contents ($n = 5$) and stool ($n = 4$) of the WT and IAP KO animals reveals that the WT animals having a significantly higher IAP enzyme activity in both their luminal contents and stool compared with the KO animals. *, $P < 0.05$, comparing WT and KO contents. (*D*) LPS-dephosphorylating activity is also much higher in the lumen and stool of the WT compared with the KO animals. *, $P < 0.05$, comparing WT and KO contents. Data in this figure are presented as mean ± SEM.

Because we showed that IAP was secreted outside of the cell *in vitro*, we sought to determine whether IAP is actively secreted into the intestinal lumen. Duodenal contents from WT and IAP KO mice were examined. We found that the WT mice had significantly higher IAP and LPS-dephosphorylating activities compared with the KO mice. Remarkably, we also found higher levels of AP and LPS-dephosphorylating activities within the stool of these WT animals (Fig. 5 *C* and *D*). Taken together, these results indicate that the IAP enzyme is secreted into the intestinal lumen by duodenal epithelial cells and that it remains functional as it is carried distally through the lumen of the small and large intestine.

Based on its ability to detoxify LPS, we hypothesized that IAP plays a role in protecting the host from luminal bacteria under pathological conditions. The mammalian small intestine is known to be very sensitive to ischemic insults, displaying a breakdown in mucosal defense against endogenous luminal bacteria/toxins (26). We have established the ischemia/reperfusion (I/R) model in our laboratory by using a standard technique of superior mesenteric artery (SMA) ligation followed by reperfusion (27) in which we also showed that the degree of mucosal injury can be titrated based on the amount of ischemia. WT and IAP KO mice were subjected to 45 min of small-intestinal ischemia followed by a variety of reperfusion times, ranging from 0 to 120 h. At specific time points, the animals were killed, and mesenteric lymph nodes were harvested to determine the degree of bacterial translocation (Fig. 6*A*). There was a small amount of background bacteria under basal conditions in both the WT and KO animals and in the control animals subjected to sham laparotomy. In response to the direct I/R injury, a dramatic increase in bacterial translocation occurs, with much higher bacterial counts in the IAP KO compared with the WT controls. Although the gut barrier became disrupted in both the WT and KO animals, it appears that the presence of IAP prevented much of the bacteria from crossing the mucosal barrier and entering the mesenteric lymph nodes. The differences were most pronounced at the 48-h time point (≈2-fold increase in bacterial counts in the KO compared with WT mice) but were also significant at the 120-h time point (≈50% increase in KO compared with WT).

In the clinical setting, gut barrier dysfunction is also known to occur in response to a variety of remote systemic insults. Accordingly, we examined the effects of IAP on gut mucosal integrity in the context of remote injury/trauma, using a model of bilateral hind-limb ischemia (2 h) followed by 24 h of reperfusion (Fig. 6*B*). Interestingly, histologic damage in hind-limb muscle and lung tissues were identical in WT and KO animals, but the degree of gut mucosal injury was much more pronounced in the IAP KO mice (see supporting information (SI) Figs. 7–10). In addition to these histological differences, we also saw a greater degree of bacterial translocation to the mesenteric nodes in the KO animals subjected to the remote leg I/R injury (≈4-fold difference between KO and WT mice in the I/R groups).

The present data indicate that IAP is a component of the gut mucosal defense system (28). IAP appears to be unique in that it is made by the enterocytes but likely exerts its protective effects at multiple locations, including inside the intestinal epithelial cell, within the intestinal lumen, and perhaps systemically. It should be noted that low levels of IAP have been detected in the bloodstream in both animals and humans (29, 30). Although the precise mechanism for IAP action *in vivo* is not yet clear, it is likely that LPS detoxification occurs at the level of the cell membrane and/or within the gut lumen.

It is likely that a similar protection against LPS may occur in other organs, whether mediated by IAP or other forms of AP. For example, Tuin *et al.* (31) studied the liver, the major LPS-removing organ in the body, and found that LPS injections enhanced AP expression in hepatocytes. Remarkably, the hepatocytes were found to take up systemically injected IAP rapidly, reducing LPS-induced damage and attenuating the LPS-induced responses *in vivo*. We speculate, therefore, that IAP is not only able to interact directly and dephosphorylate LPS within the gut, but it may also act systemically to attenuate the LPS effects in other organs. In addition, it should be noted that although liver AP is routinely measured in the clinical setting to assess the hepatic and biliary systems, the physiological function of this enzyme has never been delineated. We speculate that liver AP may function to protect the

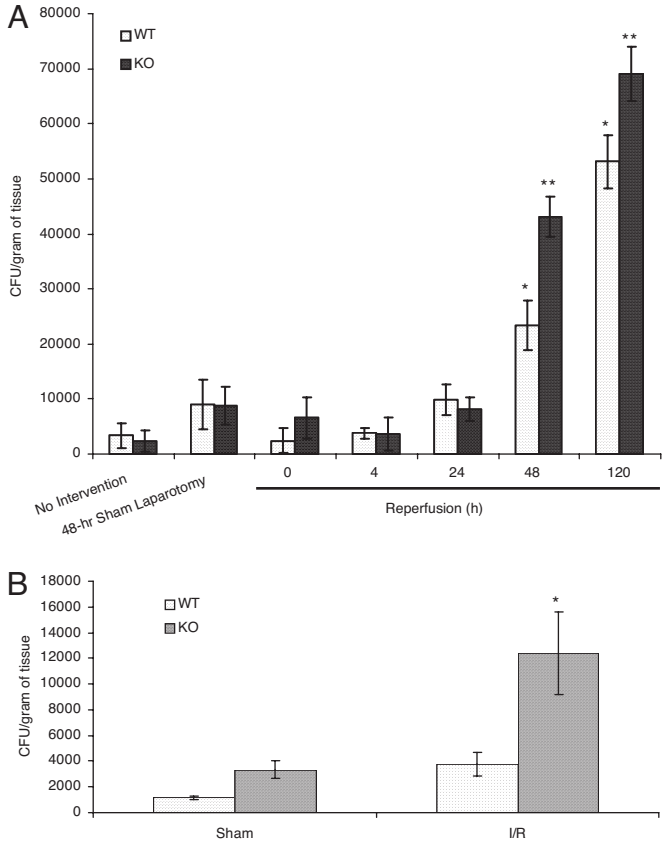

Fig. 6. IAP protects the mice from gut bacterial translocation. (*A*) Direct gut I/R. WT and IAP KO mice were exposed to 45 min of SMA clamping followed by varying times of reperfusion. Sham laparotomy and no intervention were used as controls. Mesenteric tissues were harvested, and bacterial counts in the nodes were determined. Data are based on experiments repeated on multiple occasions, $n = 4$ for no surgery, sham laparotomy, 0 and 4-h groups; $n = 7$ for 24-, 48-, and 120-h groups. *, $P < 0.05$, comparing the values with previous time points. **, $P < 0.05$, comparing KO with WT mice. (*B*) Remote trauma. After hind-limb I/R, mesenteric tissues were harvested, and bacterial counts in the nodes were determined. Sham mice were used for control purposes in all experiments. *, $P < 0.05$, comparing KO with WT mice. Data in this figure are presented as mean ± SEM.

organism from the bacteria and their toxins that may pass through the portal system.

It is intriguing to consider that the IAP silencing that occurs with starvation may at least partly explain the impaired gut mucosal defense seen in the clinical setting of critical illness. Numerous clinical studies have documented the beneficial effects of trophic enteral feeding in patients unable to tolerate a normal oral diet, but the underlying mechanisms have remained a mystery. Taken together, our data suggest that by maintaining IAP expression, enteral feeding promotes the ability of the gut to protect the host from luminal microbes and toxins such as LPS.

Materials and Methods

Details regarding plasmid construction, cell culture, RNA (RT-PCR) and protein (Western blotting) assays, transient transfections, and the creation of stable cell lines can be found in SI *Experimental Procedures*.

IAP Enzyme Activity and LPS-Dephosphorylating Assay. Kits from Upstate Biotechnology were used to assay AP enzyme activity. HT-29 cells and HT-29/IAP-overexpressing cells were first separated into their cytosolic and membranous components following the instructions in the MEM-PER eukaryotic membrane protein extraction kit from Pierce. MAPK activity was used as a control to show cytosolic activity. Also, it has been shown that sodium butyrate (NaBu) causes transactivation of the IAP gene in HT-29 cells (23), so HT-29 cells were treated with 5 mM NaBu for varying period of times to cause endogenous IAP expression. HT-29 cells overexpressing IAP (stable cells) were used for comparison as a source of ectopic IAP, and HT-29 cells not exposed to NaBu were used as a negative control. After a specific period, cells were lysed with lysis buffer [50 mM Tris·HCl (pH 7.6), 150 mM NaCl, 1 mM EDTA, 1 mM EGTA, 1% Triton X-100]. Both the fractionated cell components and lysate of all cells used *p*NPP as the substrate for the AP enzyme. As reported (32), to determine IAP activity, spectrophotometric quantitation of the hydrolyzed product of *p*NPP, *p*-nitrophenol, was used and calculated as nmol of *p*NPP hydrolyzed per minute per microgram of protein. To confirm that the AP activity was only from IAP, samples were also exposed to 10 mM phenylalanine, a known inhibitor of IAP, and 10 mM homoarginine, known to have no effect on IAP activity.

To measure the LPS-dephosphorylating activity of IAP, a protocol was established based on work described in Baykov *et al.* (33). Cell lysates from NaBu-exposed HT-29 cells and IAP overexpressing HT-29 stable cells described above were used. LPS (5 mg/ml) was added to the lysate for 2 h, then malachite green solution (0.01% malachite green, 16% sulfuric acid, 1.5% ammonium molybdate, and 0.18% Tween-20) was added and incubated for 10 min. Activity was then determined by spectrophotometric quantitation taking into account the background readings, and results were expressed in absorbance of 630 nm.

Immunohistochemical Analysis. HT-29 cells, HT-29/vector cells, and HT-29/IAP cells were all exposed ±LPS (1 μg/ml) for periods of time up to 30 min to continue our evaluation of the effects of IAP on the NF-κB pathway. After exposure to LPS, the cells were then fixed in 4% formaldehyde and then stained with RelA/p65 Ab and DAPI, as described in ref. 34. These slides were then examined under visual fields at ×400 magnification, and images were taken.

Animals. IAP KO mice (*Mus musculus* C57BL/6) construction has been described (19). Mice were obtained from the Burnham Institute for Medical Research (La Jolla, CA) and subsequently bred at the MGH animal facility to create homozygous IAP KO, heterozygous, and WT C57BL/6 littermates. Confirmation of genotype was performed by PCR analysis. Animals in this work were maintained in accordance with the guidelines of the Committee on Animals of Harvard Medical School (Boston, MA) and those prepared by the Committee on the Care and Use of Laboratory Animals of the Institute of Laboratory Resources and the National Institutes of Health (35).

***In Vivo* Test for IAP Activity and LPS-Dephosphorylating Activity.** WT and IAP KO mice, aged 8–12 weeks, were killed, and an ≈8-cm segment of bowel (starting from gastroduodenal junction and moving distally) was removed from each animal. Normal-fed animals, animals fasted for 2 days, and animals fasted for 2 days then refed for 2 days were used. Each bowel segment was then opened along its longitudinal axis and its mucosa scraped to obtain intestinal epithelial cells. By using described steps from our *in vitro* experiments, these scrapings were then lysed and exposed to *p*NPP and malachite green–molybdate solutions (see above) determining the AP activity and LPS-dephosphorylating activity, respectively.

Other WT and KO animals were killed, and the same length and location of bowel was taken to study duodenal contents. The proximal end of the bowel was attached to a syringe filled with 600 μl of normal saline (NS), and the contents were flushed into an aliquot. By using our described steps, these contents were then examined by using *p*NPP and malachite green–molybdate solutions (see above) to assess AP and LPS-dephosphorylating activities, respectively. Also, stool samples were collected from WT and KO animals, homogenized in 600 μl of NS, and assayed as well.

Intestinal I/R Injury. Surgically induced intestinal I/R has been reported (36, 37). Briefly, WT and IAP KO mice, aged 8–12 weeks, were anesthetized by i.p. injection of pentobarbital (40 mg/kg). A laparotomy was performed, followed by occlusion of the SMA with a microvascular clamp (Accurate Surgical and Scientific Instruments Corp.). After 45 min of ischemia, the microvascular clamp was removed, and the incision was reclosed. The animals were then allowed to recover from anesthesia and maintained on normal chow diet with water ad libitum. After various reperfusion times ranging between 0 and 120 h, the animals were then killed by overdose of i.p. injection of pentobarbital (200 mg/kg). A sham group underwent a similar procedure without SMA clamping, and a negative control group underwent no intervention before euthanization.

Bacterial Translocation. After euthanasia, mesenteric lymph nodes were harvested, weighed, homogenized in a specific volume of antibiotic-free LB broth, and plated on antibiotic-free agar plates to assay for bacterial growth. Fifty microliters of homogenized sample was plated onto each antibiotic-free agar plate. Plates were then left in the incubator for 24 h at 37°C. Colony-forming units

(cfu) on each plate were then counted, and each sample was normalized to cfu per gram of tissue to compensate for the varying weights of each tissue.

Hind-Limb I/R Injury. Bilateral hind-limb I/R was performed as reported (38). Briefly, WT and IAP KO mice, aged 6–8 weeks, were anesthetized by i.p. injection of pentobarbital (40 mg/kg) and subjected to 2 h of bilateral hind-limb ischemia followed by 24 h of reperfusion. For the ischemic event, tourniquets were applied above the greater trochanter using bilateral rubber bands (Latex O-rings) from the McGivney hemorrhoid ligator kit (Miltex). Control mice did not undergo banding. Mice were maintained in a supine position and kept anesthetized throughout the ischemic part of the experiment. At the conclusion of the reperfusion time, the animals were killed by pentobarbital (200 mg/kg) injection. Mesenteric lymph nodes from each animal were harvested, and using described steps the lymph nodes were assayed for bacterial growth. Bilateral hind-limb muscle fibers, bilateral lungs, duodenum, jejunum (10 cm distal to the gastroduodenal junction), and ileum were harvested, fixed, and embedded into slides and stained with Mason's Tri-Chrome to observe for histological signs of injury.

Counting the number of polymorphonuclear leukocytes present per microscopic field assessed neutrophil infiltration into the lungs, counting the number of injured muscle fibers compared with the field assessed hind-limb injury and bowel injury was assessed by using a described injury scale by Chiu *et al.* (39).

Statistical Analysis. Data are presented as the mean ± SEM or SD as specified in the figure legends. Statistical differences were determined by using two-sided independent sample Student *t* test, and a P value < 0.05 was considered statistically significant.

ACKNOWLEDGMENTS. This work was supported by National Institutes of Health Grants DK47186 and DK50623.

1. Hollander D (1999) Intestinal permeability, leaky gut, and intestinal disorders. *Curr Gastroenterol Rep* 1:410–416.
2. Nagler-Anderson C (2001) Man the barrier! Strategic defences in the intestinal mucosa. *Nat Rev Immunol* 1:59–67.
3. Muller CA, Autenrieth IB, Peschel A (2005) Innate defenses of the intestinal epithelial barrier. *Cell Mol Life Sci* 62:1297–1307.
4. Fink MP (2003) Intestinal epithelial hyperpermeability: Update on the pathogenesis of gut mucosal barrier dysfunction in critical illness. *Curr Opin Crit Care* 9:143–151.
5. Fink MP, Delude RL (2005) Epithelial barrier dysfunction: A unifying theme to explain the pathogenesis of multiple organ dysfunction at the cellular level. *Crit Care Clin* 21:177–196.
6. Gosain A, Gamelli RL (2005) Role of the gastrointestinal tract in burn sepsis. *J Burn Care Rehabil* 26:85–91.
7. Magnotti LJ, Deitch EA (2005) Burns, bacterial translocation, gut barrier function, and failure. *J Burn Care Rehabil* 26:383–391.
8. Buchman AL, *et al*. (1995) Parenteral nutrition is associated with intestinal morphologic and functional changes in humans. *J Parenter Enteral Nutr* 19:453–460.
9. Carrico CJ, Meakins JL, Marshall JC, Fry D, Maier RV (1986) Multiple-organ-failure syndrome. *Arch Surg* 121:196–208.
10. Wilmore DW, *et al*. (1988) The gut: A central organ after surgical stress. *Surgery* 104:917–923.
11. Marshall JC, Christou NV, Meakins JL (1993) The gastrointestinal tract: The ''undrained abscess'' of multiple organ failure. *Ann Surg* 218:111–119.
12. Hassoun HT, *et al*. (2001) Post-injury multiple organ failure: The role of the gut. *Shock* 15:1–10.
13. Moore EE, Jones TN (1986) Benefits of immediate jejunostomy feeding after major abdominal trauma: A prospective, randomized study. *J Trauma* 26:874–881.
14. Bengmark S, Gianotti L (1996) Nutritional support to prevent and treat multiple organ failure. *World J Surg* 20:474–481.
15. Henthorn PS, *et al*. (1987) Nucleotide and amino acid sequences of human intestinal alkaline phosphatase: Close homology to placental alkaline phosphatase. *Proc Natl Acad Sci USA* 84:1234–1238.
16. Goldstein DJ, Rogers C, Harris H (1982) Evolution of alkaline phosphatases in primates. *Proc Natl Acad Sci USA* 79:879–883.
17. Alpers DH, Mahmood A, Engle M, Yamagishi F, DeSchryver-Kecskemeti K (1994) The secretion of intestinal alkaline phosphatase (IAP) from the enterocyte. *J Gastroenterol* 29(Suppl 7):63–67.
18. Alpers DH, Zhang Y, Ahnen DJ (1995) Synthesis and parallel secretion of rat intestinal alkaline phosphatase and a surfactant-like particle protein. *Am J Physiol* 268:E1205–E1214.
19. Narisawa S, *et al*. (2003) Accelerated fat absorption in intestinal alkaline phosphatase knockout mice. *Mol Cell Biol* 23:7525–7530.
20. Beumer C, *et al*. (2003) Calf intestinal alkaline phosphatase, a novel therapeutic drug for lipopolysaccharide (LPS)-mediated diseases, attenuates LPS toxicity in mice and piglets. *J Pharmacol Exp Ther* 307:737–744.
21. Mahmood A, Shao JS, Alpers DH (2003) Rat enterocytes secrete SLPs containing alkaline phosphatase and cubilin in response to corn oil feeding. *Am J Physiol* 285:G433–G441.
22. Nguyen HT, *et al*. (2006) Proteomic characterization of lipid rafts markers from the rat intestinal brush border. *Biochem Biophys Res Commun* 342:236–244.
23. Hodin RA, Meng S, Archer S, Tang R (1996) Cellular growth state differentially regulates enterocyte gene expression in butyrate-treated HT-29 cells. *Cell Growth Differ* 7:647–653.
24. Hodin RA, Graham JR, Meng S, Upton MP (1994) Temporal pattern of rat small intestinal gene expression with refeeding. *Am J Physiol* 266:G83–G89.
25. Hodin RA, Chamberlain SM, Meng S (1995) Pattern of rat intestinal brush–border enzyme gene expression changes with epithelial growth state. *Am J Physiol* 269:C385–C391.
26. Sorkine P, *et al*. (1997) Gut decontamination reduces bowel ischemia-induced lung injury in rats. *Chest* 112:491–495.
27. Hinnebusch BF, *et al*. (2002) Enterocyte response to ischemia is dependent on differentiation state. *J Gastrointest Surg* 6:403–409.
28. McCracken VJ, Lorenz RG (2001) The gastrointestinal ecosystem: A precarious alliance among epithelium, immunity, and microbiota. *Cell Microbiol* 3:1–11.
29. Blom E, Alimm Mortensen B, Huseby NE (1998) Elimination of alkaline phosphatases from circulation by the galactose receptor: Differnt isoforms are cleared at various rates. *Clin Chim Acta* 270:125–137.
30. Meijer DK, Scholtens HB, Hardonk MJ (1982) The role of the liver in clearance of glycoproteins from the general circulation, with special reference to intestinal alkaline phosphatase. *Pharm Weekbl Sci* 4:57–70.
31. Tuin A, Huizinga-Van der Vlag A, van Loenen-Weemaes AM, Meijer DK, Poelstra K (2006) On the role and fate of LPS-dephosphorylating activity in the rat liver. *Am J Physiol* 290:G377–G385.
32. Malo MS, *et al*. (2006) The proinflammatory cytokines, IL-1β and TNF-α, inhibit intestinal alkaline phosphatase gene expression. *DNA Cell Biol* 25:684–695.
33. Baykov AA, Evtushenko OA, Avaeva SM (1988) A malachite green procedure for orthophosphate determination and its use in alkaline phosphatase-based enzyme immunoassay. *Anal Biochem* 171:266–270.
34. Jobin C, *et al*. (1999) Curcumin blocks cytokine-mediated NF-κB activation and proinflammatory gene expression by inhibiting inhibitory factor I-κB kinase activity. *J Immunol* 163:3474–3483.
35. Committee on Care and Use of Laboratory Animals (1985) *Guide for the Care and Use of Laboratory Animals* (Natl Inst Health, Bethesda), DHHS Publ No (NIH) 85-23.
36. Williams JP, *et al*. (1999) Intestinal reperfusion injury is mediated by IgM and complement. *J Appl Physiol* 86:938–942.
37. Zhang M, *et al*. (2004) Identification of a specific self-reactive IgM antibody that initiates intestinal ischemia/reperfusion injury. *Proc Natl Acad Sci USA* 101:3886–3891.
38. Crawford RS, *et al*. (2007) A novel model of acute murine hindlimb ischemia. *Am J Physiol* 292:H830–H837.
39. Chiu CJ, McArdle AH, Brown R, Scott HJ, Gurd FN (1970) Intestinal mucosal lesion in low-flow states. I. A morphological, hemodynamic, and metabolic reappraisal. *Arch Surg* 101:478–483.